Papers, volume 5 - 1997-2000

Thoft-Christensen, Palle

CHAPTER 93

WIND TUNNEL EXPERIMENTS WITH ACTIVE CONTROL OF BRIDGE SECTION MODEL[1]

H.I. Hansen & P. Thoft-Christensen
Aalborg University, Aalborg, Denmark

SUMMARY

This paper describes results of wind tunnel experiments with a bridge section model where movable flaps are integrated in the bridge girder so each flap is the streamlined part of the edge of the girder. This active control flap system is patented by COWIconsult [1] and may be used to increase the flutter wind velocity for future ultra-long span suspension bridges. The purpose of the wind tunnel experiments is to investigate the principle to use this active flap control system. The bridge section model used in the experiments is therefore not a model of a specific bridge but it is realistic compared with a real bridge. Five flap configurations are investigated during the wind tunnel experiments and depending on the actual flap configuration it is possible to decrease or increase the flutter wind velocity for the model.

1. INTRODUCTION

During the last decades the span length of suspension bridges has grown rapidly. During 1998 two very long suspension bridges are planned to be opened for traffic, namely the Akashi Kaikyo Bridge in Japan with span length 1,991 m and the Great Belt Bridge in Denmark with span length 1,624 m. Of future ultra-long span suspension bridges that may be constructed can be mentioned the Messina Crossing with the span length 3,300 m and the crossing of the Gibraltar Straits, see Brown [4].

To increase the span length the suspension bridge can be optimised with regard to materials, deck shape and cables as described by Brown [4), Gimsing [7], Astiz [3], Ostenfeld [10] and Ostenfeld & Larsen [11]. Another possibility may be to introduce the intelligent bridge, where active control systems are used to limit the vibrations. A

[1] Proceedings IABSE Symposium on “Long-Span and High-Rise Structures”, Kobe, Japan, September 1998, pp. 199-204.

step in this direction is to introduce passive control systems, e.g. viscoelastic damping elements, tuned mass dampers and eccentric masses, as described by Ostenfeld & Larsen [11]. In advanced aircrafts actively controlled surfaces are moved relatively to the main surfaces (wings, flaps or ailerons) on which they exert control [11]. The control surfaces are moved by hydraulics based on measurements from sensors attached to the main surfaces. The same principle could be applied to bridges as patented by COW/consult [1].

2. WIND LOADS

For ultra-long span suspension bridges the main aeroelastic effect of concern is flutter; see Astiz [3] and Larsen & Walther [9]. In flutter the motion-induced wind load is dominating the wind load. Flutter occurs at a critical wind velocity at which the energy input from the motion-induced wind load is equal to the energy dissipated by structural damping; see Dyrbye & Hansen [5]. The critical wind velocity is called the flutter wind velocity.

The motion-induced wind loads on a streamlined bridge deck with integrated flaps can be described by aerodynamic derivatives. For new bridge designs these coefficients must be estimated by wind tunnel tests or by numerical flow simulations. For flexible bridges the cross-sectional shape of the bridge deck is the most dominating factor on the wind loads, see Scanlan [12). Therefore, bridge section models are used to estimate the aerodynamic derivatives. During preliminary bridge design the aerodynamic derivatives may be approximated by the values for a flat plate. Theodorsen [13] has derived the force and moment on a flat plate with a trailing flap. This context can be extended to include the leading flap by assuming that the rotation of the leading flap has no effect on the circulation. The results of the wind tunnel experiments are compared with the theoretical results for a flat plate with both leading and trailing flaps.

3. TEST SET-UP

Experiments have shown that the critical wind velocity for a streamlined girder is much higher than for a rectangular girder, see Ostenfeld & Larsen [11]. The bridge section model is therefore made streamlined with the flaps as the streamlined part. The cross-sectional shape of the model equipped with flaps is shown in figure 1. The width of the model exclusive flaps is B, the height of the model is 0.15 B and each of the flaps has the length 0.25 B.

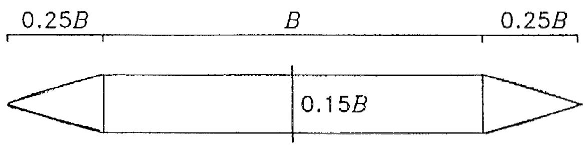

Figure 1. Cross-sectional shape of bridge.

Scaling factor	Symbol	Value
Length	λ_L	1/40
Wind velocity	λ_V	1/4
Mass density of surroundings	λ_ρ	1

Table 1. Selected scaling factors.

The selected scaling factors and the parameters for the model are shown in table 1 and 2, respectively.

Parameter	Symbol	Value
Width of model inclusive flaps	B	0.937 m
Mass per unit length	m	17.94 kg/m
Mass moment of inertia per unit length	I	0.589 kg m^2/m
Circular frequency for bending	ω_z	5.2 rad/s
Circular frequency for torsion	ω_α	10.1 rad/s
Structural damping in bending	ζ_z	0.012
Structural damping in torsion	ζ_α	0.008

Table 2. Parameters for bridge section model.

The model is connected to a horizontal extension rod in each side which is going through the wind tunnel wall. The suspension system is the same in both sides. The extension rod is connected to an arm with dummy masses that can be moved on the arm so the model can represent the correct mass and mass inertia. Each side of the arm is suspended in a helical spring. The springs can be moved on the arm so the stiffness corresponding to the torsional motion of the model can be adjusted. Finally the extension rod is connected to a windward drag wire and a leeward drag wire. A simplified illustration of one side of the suspension system is shown in figure 2.

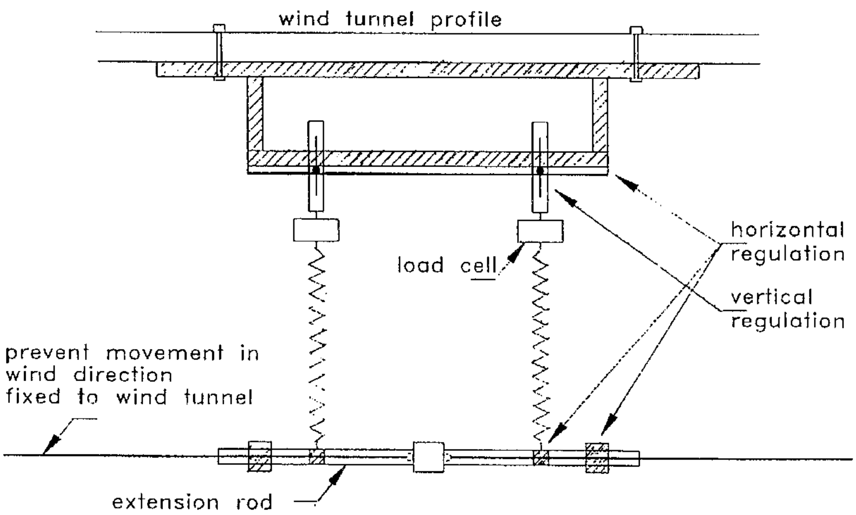

Figure 2: Simplified suspension system.

The active flap control system consists of:

- Load cells to measure the position of the model.
- Calculation of flap positions based on the position of the model and the flap configuration.
- Servo system with servo amplifiers, servo motors and reduction gears to regulate the flaps via cables between the gears and the flaps. This system consists of two separate parts as the flaps can be regulated independently.

4. WIND TUNNEL EXPERIMENTS

The positive definitions of the vertical position z, the torsional angle α, the angle of the leading flap α_l and the trailing flap α_t are shown in figure 3. *U* is the mean wind velocity.

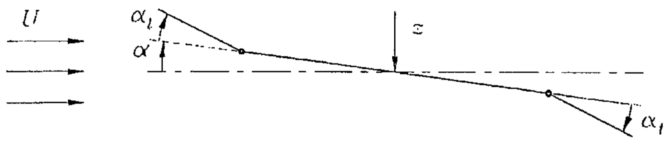

Figure 3. Definition of positive directions.

The torsional motion can be described by

$$\alpha(t) = A_\alpha(t)\cos(\omega'_\alpha t) \quad (1)$$

where t is the time, $A_\alpha(t)$ is the amplitude of the envelope curve for the torsional motion and ω'_α is the circular eigenfrequency for the damped torsional motion. The actual flap position for e.g. the trailing flap can be described by

$$\alpha(t) = a_t A_\alpha(t)\cos(\omega'_\alpha t - \varphi_t) \quad (2)$$

here a_t is the amplification factor and φ_t is the phase angle for the trailing flap. In the same way the actual flap position for the leading flap can be described by the amplification factor a_l and the phase angle φ_l.

$$\alpha(t) = a_l A_\alpha(t)\cos(\omega'_\alpha t - \varphi_l) \quad (3)$$

The amplification factors and phase angles for the flap configurations are shown in table 3.

Flap configuration	Amplification		Phase angles	
	a_t	a_l	φ_t [rad]	φ_l [rad]
0	0	0	-	-
1	1.9	-2.0	4.5	4.5
2	3.4	-3.6	4.6	4.6
3	2.0	-2.0	1.5	1.5
4	3.4	-3.6	1.5	1.5

Table 3: Amplification factors and phase angles for each flap configuration.

A damping experiment follows the procedure:

1. Justification of wind velocity.
2. The model is given a “standardised” initial displacement by pulling a rope that is connected to the horizontal arms of the model.
3. Start of the program that measures the position of the model every 12 m.
4. The flaps are started slowly at the first upcrossing of the torsional motion with the desired flap configuration. The actual positions of the flaps are measured and new values are specified every 12 m.
5. The results are stored and used to estimate the damping of the model from the free vibration following the initial displacement.

The damping ratio for the torsional motion as a function of the wind velocity is estimated based on the wind tunnel experiments. The damping ratio can also be estimated by the Air Material Command method, see e.g. Fung [6]. The damping ratio $g(U)$ defined in the AMC method as twice the necessary structural damping is replaced by $-0.5\, g(U) + 0.008$ to be compared with the experimental damping ratios.

The damping ratios estimated based on the experimental data are compared to the theoretical damping ratios by using the AMC method and the aerodynamic derivatives for a flat plate for flap configurations 0-4, see figure 4.

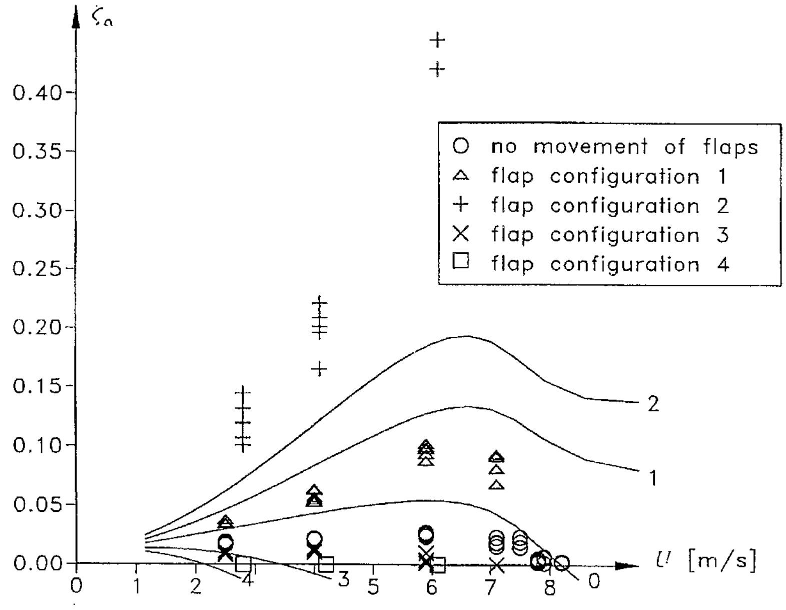

Figure 4: Theoretical (solid lines) and experimental damping ratio for torsional motion with wind for flap configuration 0-4. The number in the end of a solid line denotes the actual flap configuration.

As seen in figure 4 the experimental damping ratio is smaller for flap configurations 0 and 1 than the theoretical damping ratio but the shape of the curve is almost the same. For flap configuration 2 the experimental damping ratio exceeds the theoretical one. For flap configurations 1 and 2 the theoretical curves show that no binary flutter will occur. Unfortunately, it was not possible during the wind tunnel experiments to perform experiments with wind velocities above the relatively low divergence wind velocity (8.5 m/s) without the risk to damage the model.

5. CONCLUSIONS

The wind tunnel experiments show that it is possible by using very simple closed-loop control algorithms for the active flap control system to increase or decrease the flutter wind velocity for the bridge section model. The control algorithms are not optimised with regard to the amplification factors and phase angles, it is therefore expected that the effect of the flaps can be even better.

6. ACKNOWLEDGEMENT

The present research was supported by The Danish Technical Research Council within the research program “Safety and Reliability”.

BIBLIOGRAPHY

[1] European Patent Specification. A System and a Method of Counteracting Wind induced Oscillations in a Bridge Girder. EP 0 627 031 B 1. Bulletin 1996/24.
[2] Proceedings of the 15th Congress of IABSE. Copenhagen, Denmark, June 16-20, 1996.
[3] M.A. Astiz. Wind Related Behaviour of Alternative Suspension Systems. In [2], p.1079-1090.
[4] W.C. Brown. Development of the Deck for the 3300 m Span Messina Crossing. In [2], pp.1019-1030.
[5] C. Dyrbye and S.O. Hansen. Wind Load on Structures. John Wiley & Sons, 1996.
[6] Y.C. Fung. An Introduction to the Theory of Aeroelasticity. John Wiley & Sons, 1955.
[7] N.J. Gimsing. Large Bridges of the Future. In [8], pp. 295-304.
[8] A. Larsen, editor. Aerodynamics of Large Bridges, Proceedings of the First International Symposium on Aerodynamics of Large Bridges, Copenhagen, Denmark, 1992.
[9] A. Larsen and J.H. Walther. A New Computational Method for Assessment of the Aeroelastic Stability of Long Span Bridges. In [2], pp. 93-98.
[10] K.H. Ostenfeld. Comparison between different Structural Solutions. The Great Belt Project. In [2], pp. 1063-1078.
[11] K.H. Ostenfeld and A. Larsen. Bridge Engineering and Aerodynamics. In [8], pp. 3-22.
[12] R.H. Scanlan. Wind Dynamics of Long-Span Bridges. In [8], pp. 47-57.
[13] T. Theodorsen. General Theory of Aerodynamic, Instability and the Mechanism of Flutter, p. 22-31. AIAA Selected Reprint Series, Vol. V, Aerodynamic Flutter. American Institute of Aeronautics and Astronautics, 1976. NACA Rep. No. 496 (1935).